Spin Transition Zone in Earth's Lower Mantle

Jung-Fu Lin,[1] György Vankó,[2,3] Steven D. Jacobsen,[4] Valentin Iota,[1] Viktor V. Struzhkin,[5] Vitali B. Prakapenka,[6] Alexei Kuznetsov,[6] Choong-Shik Yoo[1*]

Mineral properties in Earth's lower mantle are affected by iron electronic states, but representative pressures and temperatures have not yet been probed. Spin states of iron in lower-mantle ferropericlase have been measured up to 95 gigapascals and 2000 kelvin with x-ray emission in a laser-heated diamond cell. A gradual spin transition of iron occurs over a pressure-temperature range extending from about 1000 kilometers in depth and 1900 kelvin to 2200 kilometers and 2300 kelvin in the lower mantle. Because low-spin ferropericlase exhibits higher density and faster sound velocities relative to the high-spin ferropericlase, the observed increase in low-spin (Mg,Fe)O at mid-lower mantle conditions would manifest seismically as a lower-mantle spin transition zone characterized by a steeper-than-normal density gradient.

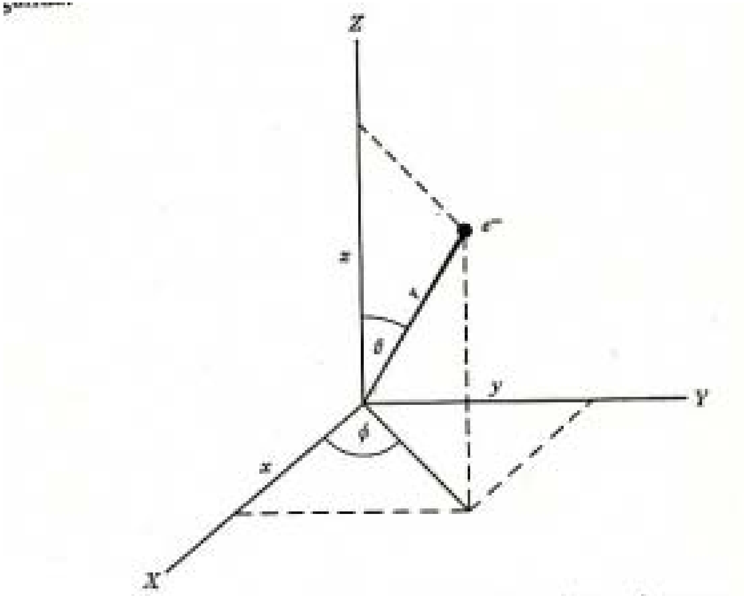

FIGURE 2.1 Polar co-ordinates of an electron in space.

Orbital wave function for electron:

$\Psi(r,\theta,\phi) = R(r)\cdot\Theta(\theta)\cdot\Phi(\phi)\cdot\Psi_s$

R(r): radial function

$\Theta(\theta)$, $\Phi(\phi)$: angular functions

Ψ_s: spin function

Quantum numbers:

n: the principal quantum number from R(r), 1, 2, …n

l: the azimuthal quantum number related to the shape of an orbit, *l*: 0, 1, 2,…(n-1)

m_l: the magnetic quantum number, the directions of maximum extension in shape of the electron cloud, -*l*,….0,….,*l*

m_s: spin quantum number, 1/2 (clockwise), -1/2 (anticlockwise)

Angular distribution probabilities for electrons in *s*, *p*, and *d* orbitals.

Lobes.

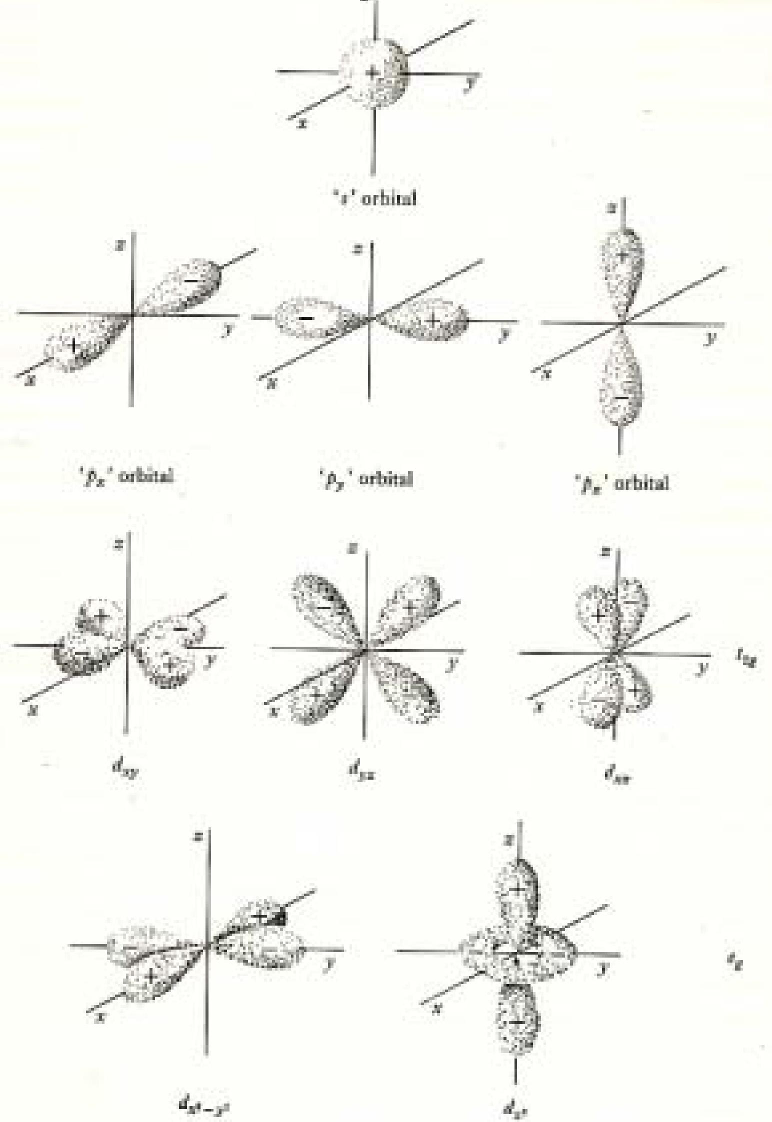

FIGURE 2.2 Boundary surfaces of atomic orbitals.

The boundaries represent angular distribution probabilities for electrons in each orbital. The sign of each wave function is shown. The *d* orbitals have been classified into two groups, t_{2g} and e_g, on the basis of spatial configuration with respect to the cartesian axes. (Reproduced and modified from: W. S. Fyfe, *Geochemistry of Solids*, McGraw-Hill Book Co., New York, 1964, figure 2.5, p. 19.)

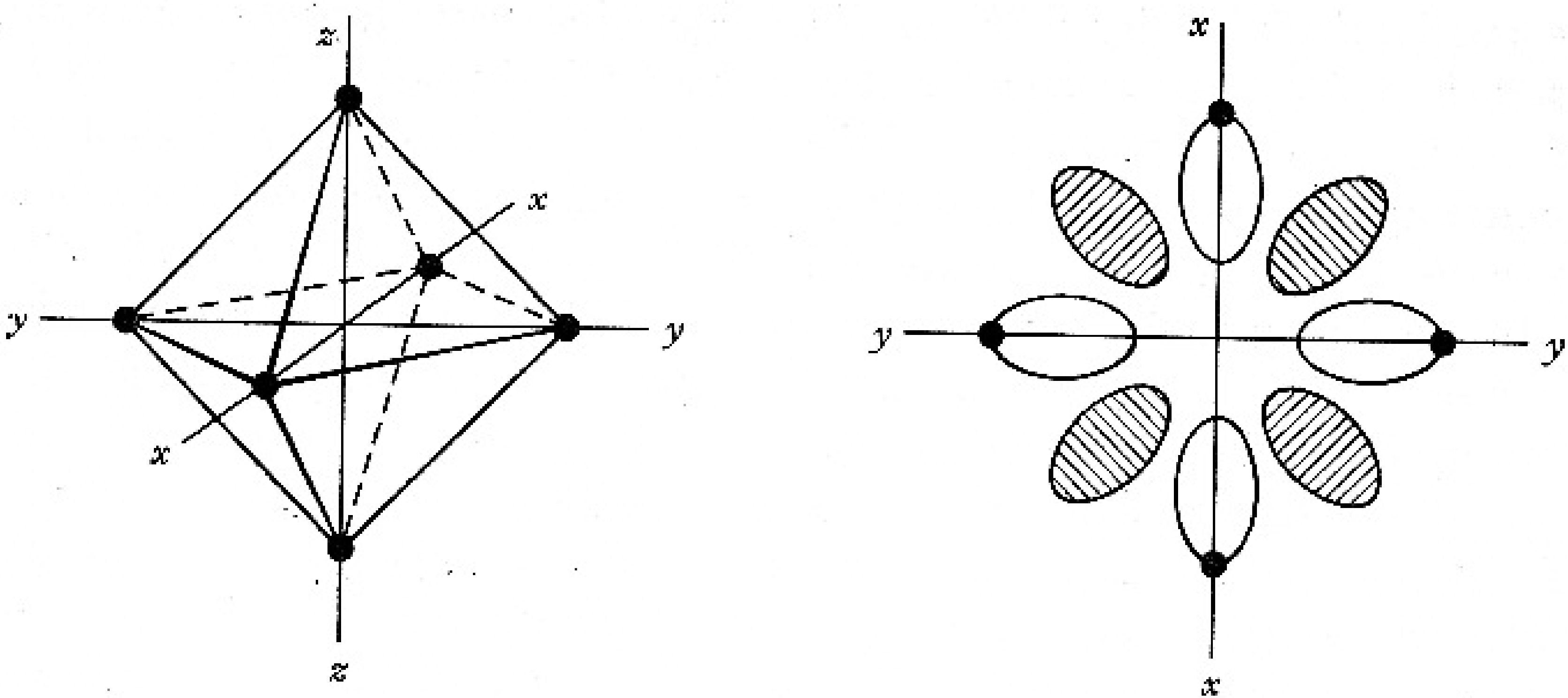

(a) (b)

FIGURE 2.3 Orientations of ligands and d orbitals of a transition metal ion in octahedral co-ordination (a) orientation of ligands with respect to the cartesian axes; (b) the x–y plane of a transition metal ion in an octahedral crystal field. d_{xy} orbital is crosshatched; $d_{x^2-y^2}$ orbital is open; ligands are black circles.

Spin state of Fe^{2+} (d^6) in octahedral coordination

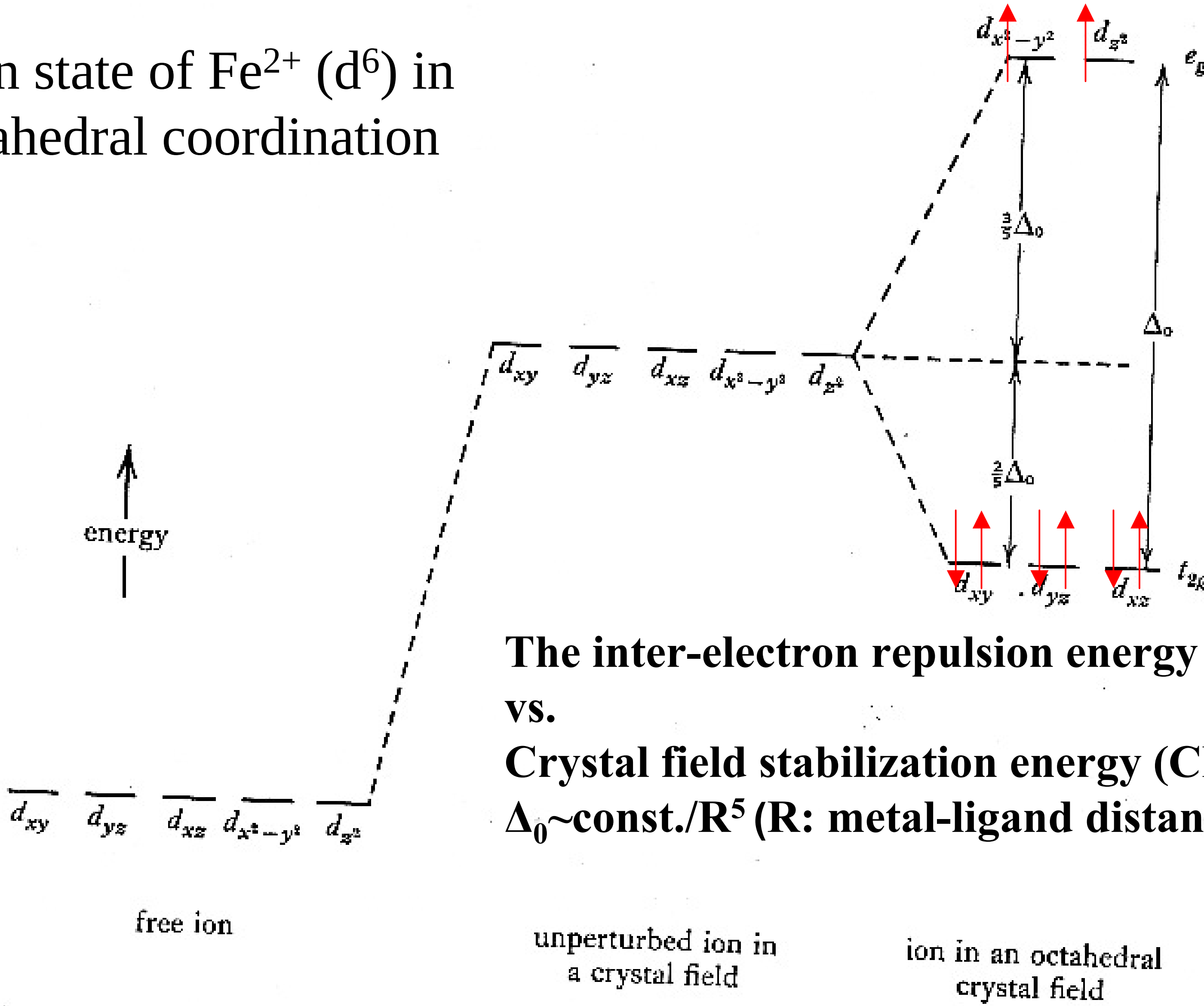

The inter-electron repulsion energy

vs.

Crystal field stabilization energy (CFSE)

Δ_0~const./R^5 (R: metal-ligand distance)

FIGURE 2.4 Relative energy levels of *d* orbitals of a transition metal ion in octahedral co-ordination.

General haracteristics of transition metal ion in the low spin state:

+ smaller effective ionic radius, or smaller volume

+ higher elastic modulii

+ smaller magnetic moment

+ etc.

++ Reduction of radiative conductivity of low-spin Fp (Goncharov et al., 2006)

Sound velocities if Fp in lower mantle condition measure by nuclear resonant inelastic X-ray scattering to 110 GPa.

Lin et a., 2006

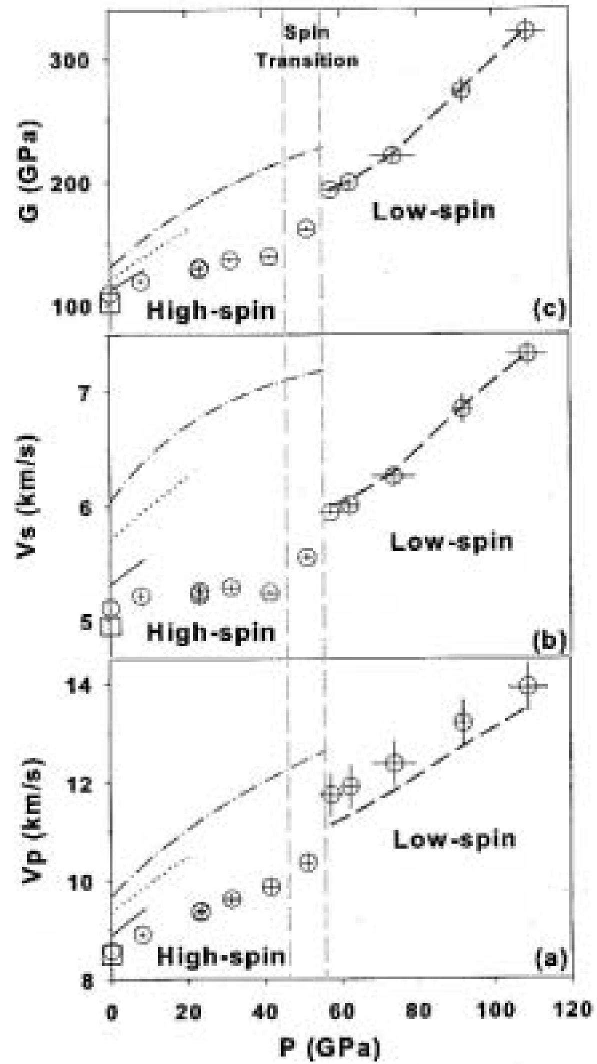

Figure 2. Aggregate (a) V_P, (b) V_S, and (c) G of $(Mg_{0.75}, Fe_{0.25})O$ at high pressures. Open circles: this study based on the Birch-Murnaghan EOS [*Birch*, 1986] of *Lin et al.* [2005]; Dashed lines: this study based on the K_S and its pressure derivative of MgO with the density of $(Mg_{0.75}, Fe_{0.25})O$ [*Fei et al.*, 2005]; Dash-dotted lines: V_P, V_S, and G of MgO [*Zha et al.*, 2000]; Dotted lines: $(Mg_{0.94}, Fe_{0.06})O$ from Brillouin measurements [*Jackson et al.*, 2006]; Solid lines: $(Mg_{0.83},$

Spin Transition Zone in Earth's Lower Mantle

Jung-Fu Lin,[1] György Vankó,[2,3] Steven D. Jacobsen,[4] Valentin Iota,[1] Viktor V. Struzhkin,[5] Vitali B. Prakapenka,[6] Alexei Kuznetsov,[6] Choong-Shik Yoo[1*]

Mineral properties in Earth's lower mantle are affected by iron electronic states, but representative pressures and temperatures have not yet been probed. Spin states of iron in lower-mantle ferropericlase have been measured up to 95 gigapascals and 2000 kelvin with x-ray emission in a laser-heated diamond cell. A gradual spin transition of iron occurs over a pressure-temperature range extending from about 1000 kilometers in depth and 1900 kelvin to 2200 kilometers and 2300 kelvin in the lower mantle. Because low-spin ferropericlase exhibits higher density and faster sound velocities relative to the high-spin ferropericlase, the observed increase in low-spin (Mg,Fe)O at mid-lower mantle conditions would manifest seismically as a lower-mantle spin transition zone characterized by a steeper-than-normal density gradient.

Electronic spine state of Fe in Fp $(Mg_{0.75}Fe_{0.25})O$ and its crystal structure were studied up to 95 GPa and 2000 K with a LHDAC.

The samples were [110] oriented crystal plates or polycrystalline samples of $(Mg_{0.75}Fe_{0.25})O$, 12 μm thick and 70 μm in diameter. Samples were sandwiched by dried NaCl layer in DAC with Be gasket.

The spin state were proved by in situ x-ray emission spectroscopy (XES). A Rowland circle spectrometer with 1-m diameter was configured around the double-side laser-heating system at APS. The Fe fluorescence lines were excited by 14 keV x-ray beam focused down to ca. 5 μm at the sample position. The XES spectra of the Fe Kβ line were collected by a silicon detector through the Be gasket and a Si(333) analyzer.

Fig. 2. Representative angle-dispersive x-ray diffraction patterns of $(Mg_{0.75},Fe_{0.25})O$ at ~84 GPa and high temperatures collected from a laser-heated diamond cell. A monochromatic beam of 0.3344 Å in wavelength was used as the x-ray source, and the diffracted x-rays were collected by an image plate (MAR345). The diffraction patterns were integrated with the FIT2D program, and the backgrounds were subtracted for clarity. $(Mg_{0.75},Fe_{0.25})O$ is stable in the B1 structure up to 1900 K and remains in the B1 structure after hours of laser heating (*26*). Fp, $(Mg_{0.75},Fe_{0.25})O$; NaCl, thermal insulator in the B2 structure. Temperature uncertainties in the experiments were approximately 100 to 150 K. Optical observation of the laser-heated sample shows no evidence of a phase separation.

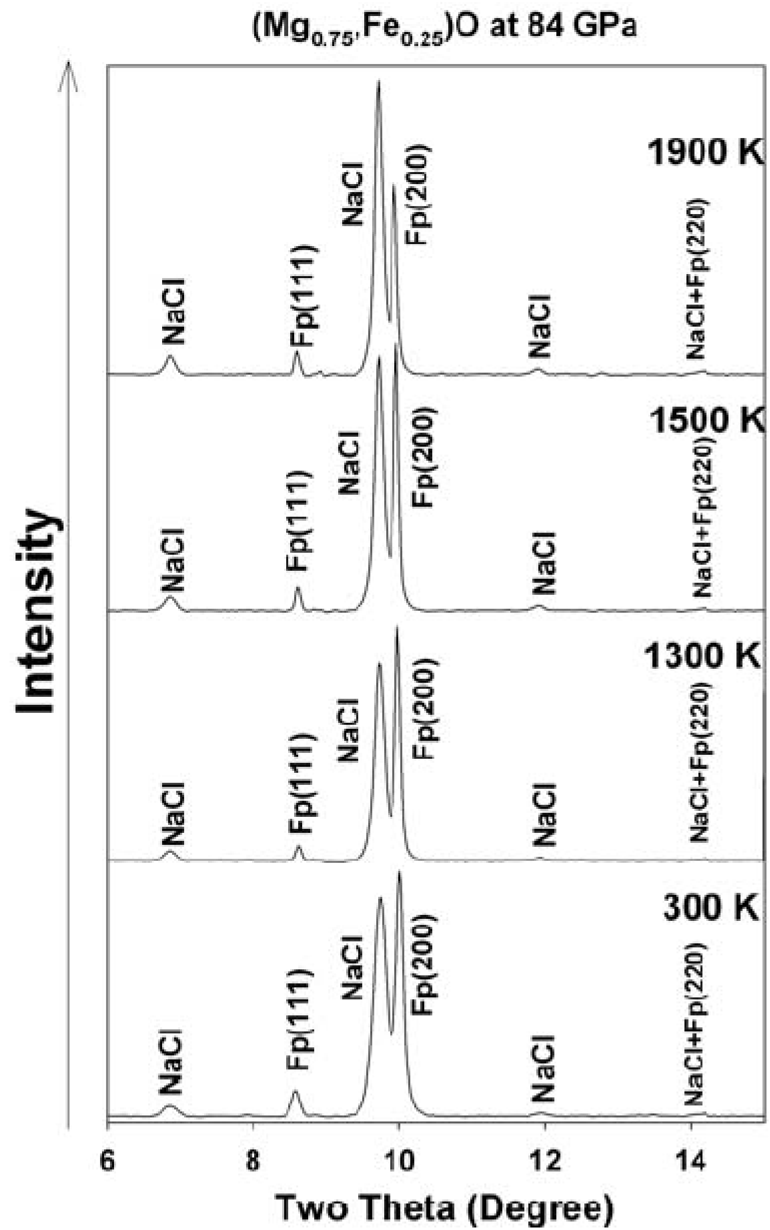

The high-spin **Fp** assumes the **B1** structure.

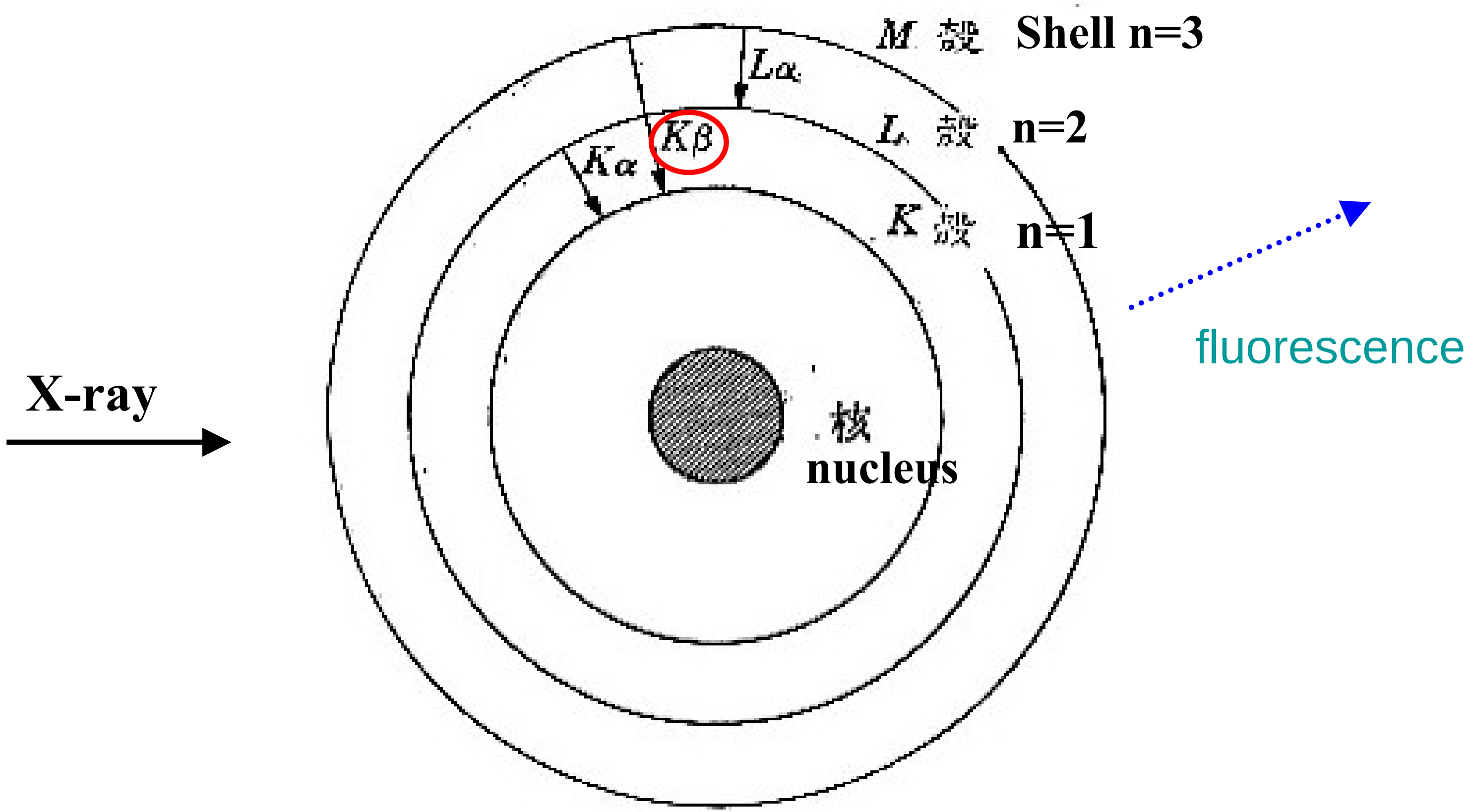

図 1-7　原子内での電子の移行．X線の放出は矢印で示されている．

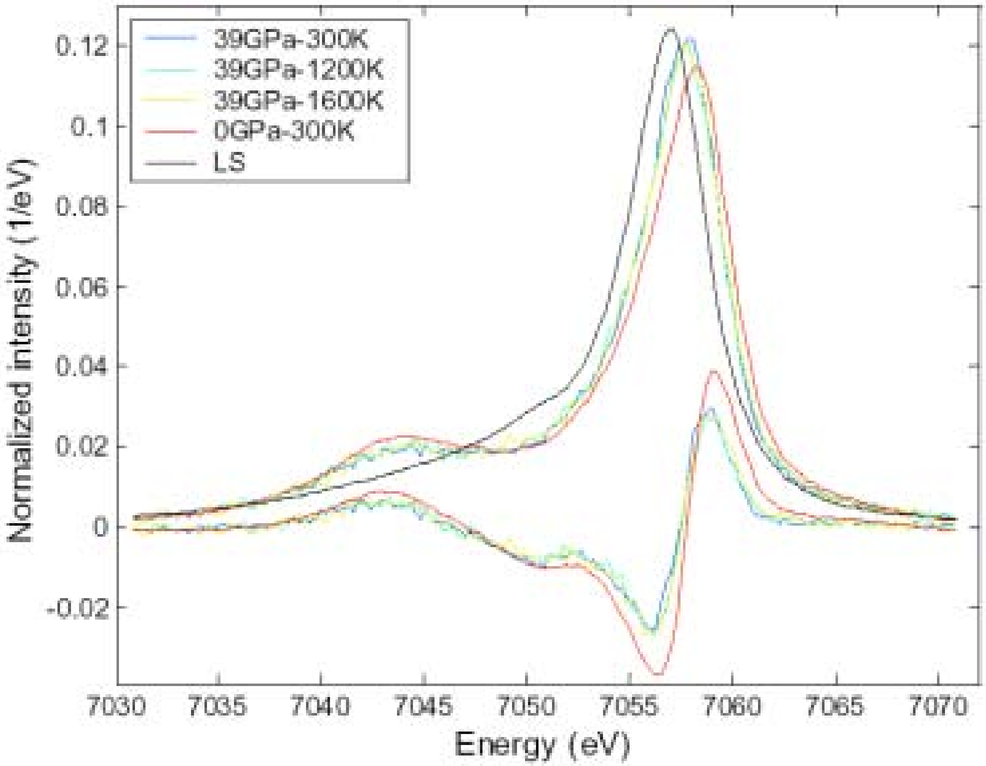

Fig. S1. Representative x-ray emission spectra of Fe Kβ collected from ferropericlase-$(Mg_{0.75},Fe_{0.25})O$ at 39 GPa and high temperatures. X-ray emission spectra collected at ambient pressure and 80 GPa are used as references for the IAD analysis (*S6*) of the high-spin and low-spin states, respectively. Differences from the low-spin line shape, shown below the spectra, are used to derive the ratio of the high-spin to low-spin states in the sample.

The satellite intensity is increased at higher spin, which is supported by theoretical considerations (“should be S/(S+1) times that of the main peak”). Thus qualitative analysis could be OK.

Analysis of XES to derive HS/LS ratio (integrated absolute disffrence (IAD) analysis):

Let us note the HS and XE spectral functions a ***h*(*E*)** and ***l(E)*** , respectively , which are normalized to unit area at integration. The **IAD** value for the complete spin transition can be given as $\mathbf{IAD_{HL}} = \int | h(E) - l(E) | \, dE$. A spectrum of in the transitional region is a superposition of those of the two spinstates, thus it can be expresses as $s = \gamma_{HS} h + (1 - \gamma_{HS} h) l$. The integrals of its absolute value is

$$\mathbf{IAD(s)} = \int | s(E) - l(E) | \, dE = \gamma_{HS} \, \mathbf{IAD_{HL}}.$$

γ_{HS}: proportion in the high spin state

The reference can be the HS spectrum as well or any linear combination of the two spectra.

Fig. 1. Representative x-ray emission spectra of Fe Kβ collected from ferropericlase-$(Mg_{0.75},Fe_{0.25})O$ at high pressures and temperatures. (**A**) 51 GPa and high temperatures; (**B**) 80 GPa and high temperatures. High-quality XES spectra collected at ambient pressure and 80 GPa are used as references for the IAD analysis (*23*) of the high-spin and low-spin states, respectively. Differences from the low-spin line shape, shown below the spectra, are used to derive the ratio of the high-spin to low-spin states in the sample. An energy shift of ~1.6 eV in the main emission peak (Kβ) can also be seen across the spin transition.

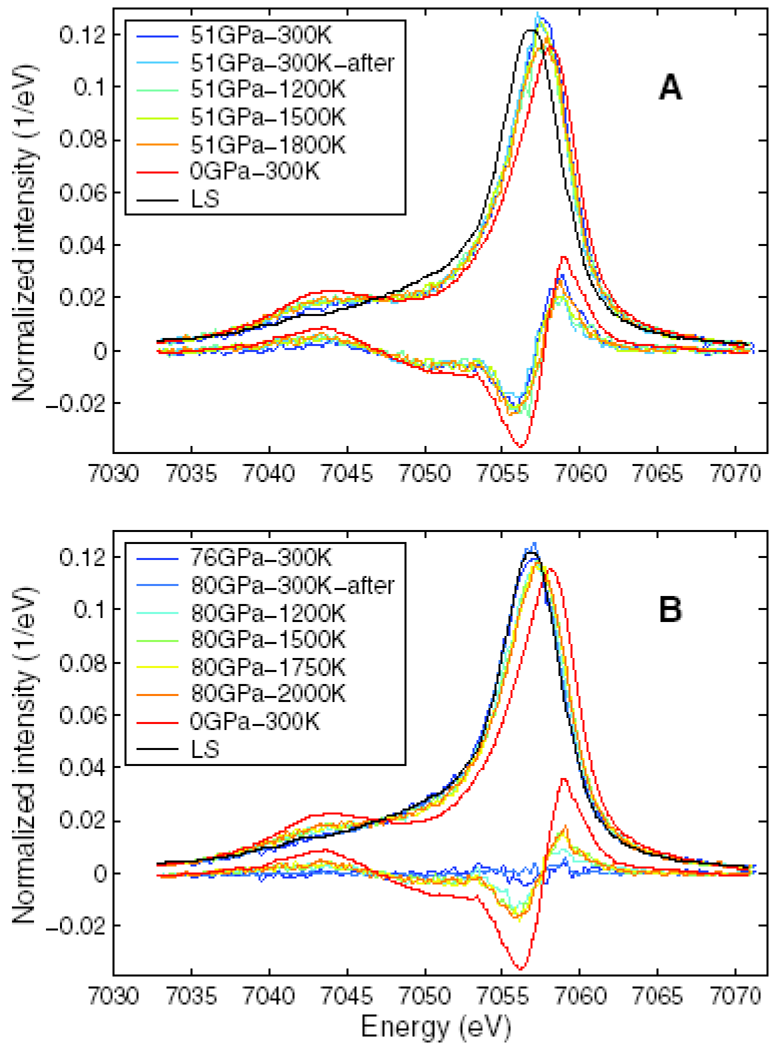

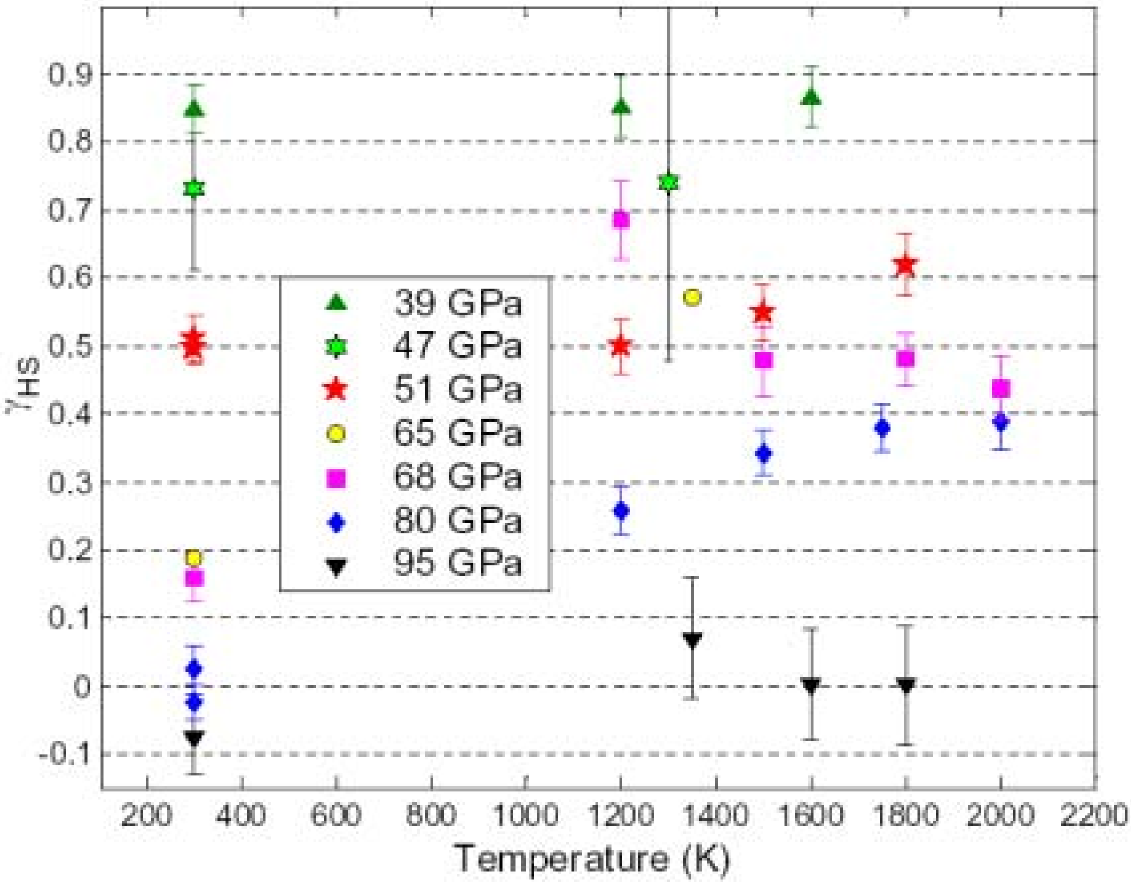

Fig. S2. Fractions of the high-spin iron in $(Mg_{0.75},Fe_{0.25})O$ at high pressures and temperatures. The high-spin fraction, γ_{HS}, is derived from the line shape analysis of the X-ray emission spectra (*S6*) collected at high pressures and temperatures (Fig. 1). The large error bars ($\pm 1\sigma$) at 47 GPa and 1300 K arise from the low statistics of the XES spectrum.

Fig. 3. Isosymmetric spin crossover of Fe^{2+} in $(Mg_{0.75},Fe_{0.25})O$. The phase diagram is constructed from the interpolation and extrapolation of the derived fractions of the high-spin state in the sample (fig. S2). Colors in the vertical column on the right represent fractions of the high-spin iron, γ_{HS}, in $(Mg_{0.75},Fe_{0.25})O$.

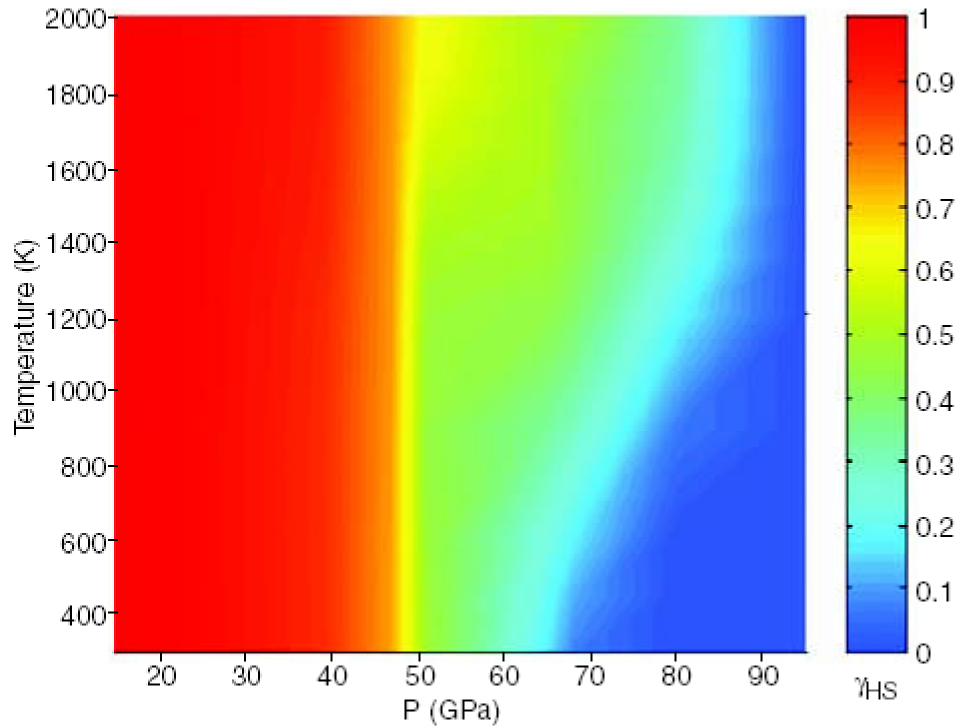

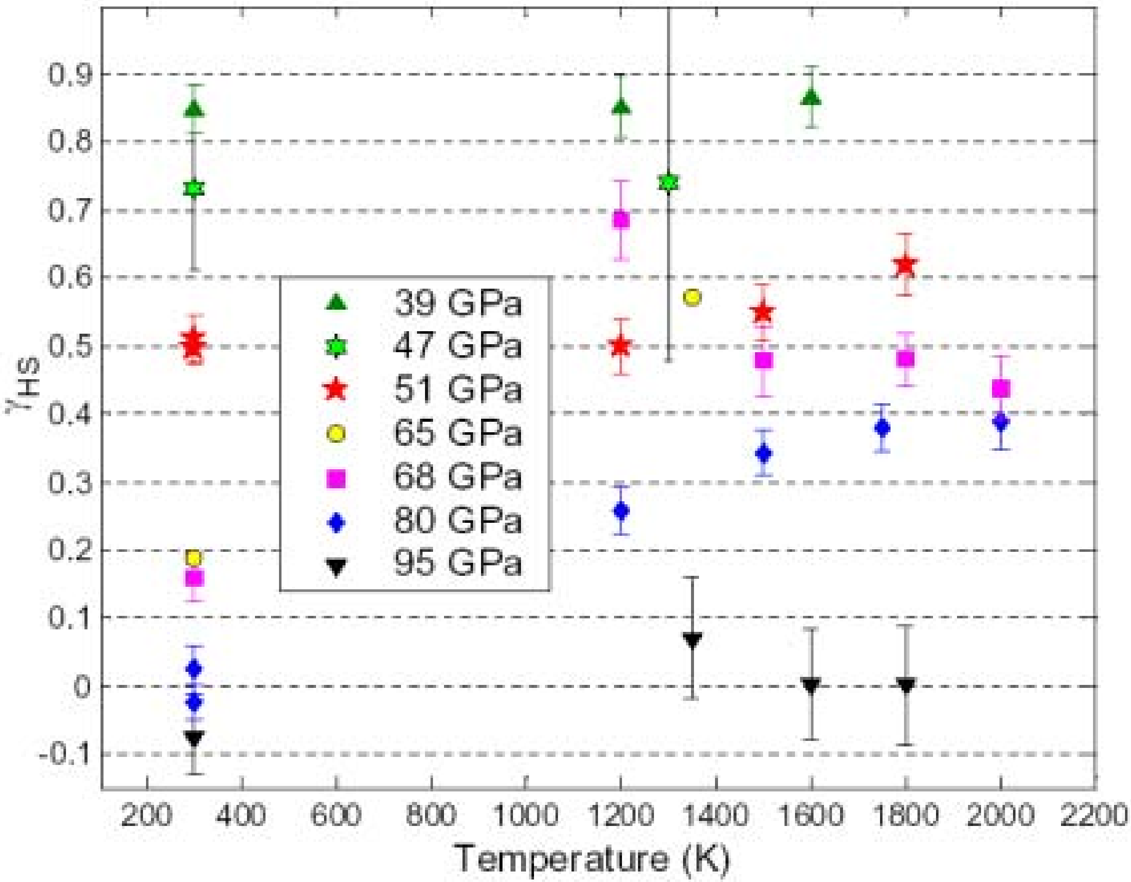

Fig. S2. Fractions of the high-spin iron in $(Mg_{0.75},Fe_{0.25})O$ at high pressures and temperatures. The high-spin fraction, γ_{HS}, is derived from the line shape analysis of the X-ray emission spectra (*S6*) collected at high pressures and temperatures (Fig. 1). The large error bars ($\pm 1\sigma$) at 47 GPa and 1300 K arise from the low statistics of the XES spectrum.

Adiabatic temperature profiles in the Earth

Brown and Shankland, 1981.

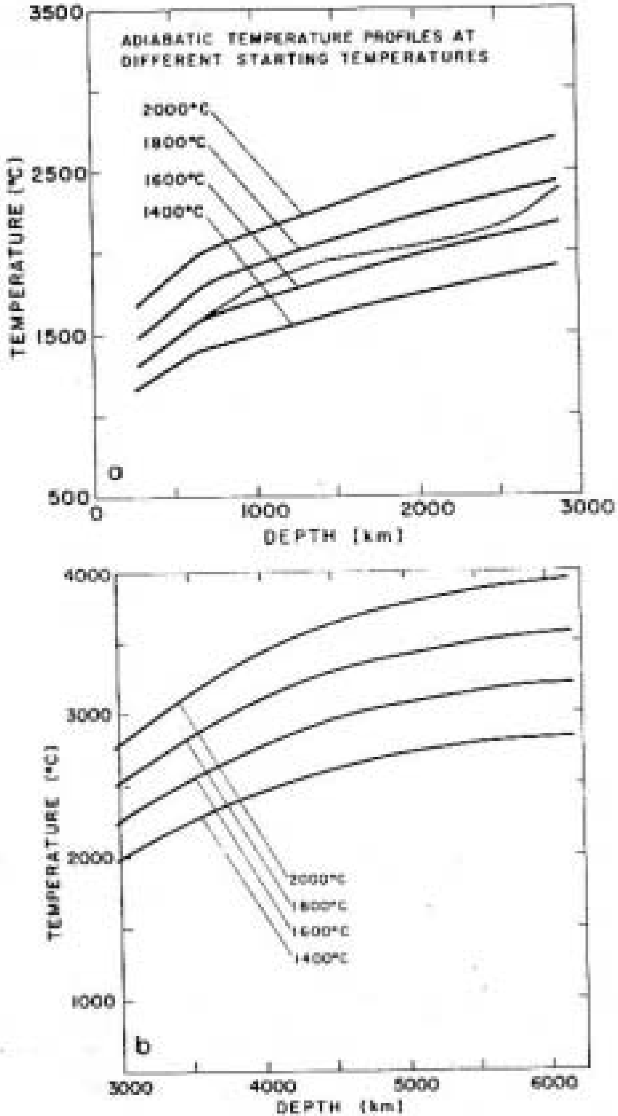

Figure 2. Adiabatic temperature profiles (a) in the mantle and (b) in the core. The curves have been constructed for the four different indicated temperatures at 670 km depth. The second curve beginning at 1600°C and 670 km includes the calculated superadiabatic contribution.

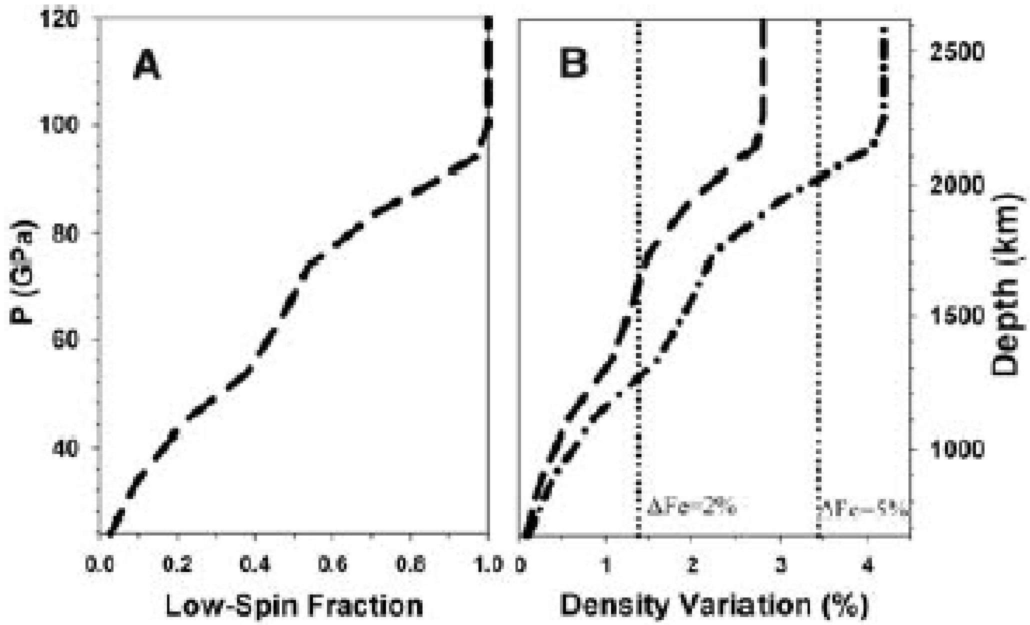

Fig. 4. Derived fractions of the low-spin ferropericlase (**A**) and density variation (**B**) along a model lower-mantle geotherm (*20*). Fraction of the low-spin ferropericlase is derived from an extrapolation of the experimental data in Fig. 3. Density variations in ferropericlase across the spin-crossover region assume that the density varies linearly with the fraction of the low-spin iron (*22*). Dashed line and dash-dotted line represent derived density variations using maximum variations of 2.8% and 4.2% across the spin-crossover region from evaluation of recent experimental (*5*) and theoretical (*11*) data, respectively. Vertical bars represent the density variations caused by 2% and 5% perturbation of total iron content in ferropericlase, respectively, at ambient conditions (*32*).

Summary:

Spin state of iron in ferropericlase have been measure up to 95 GPa and 2000 K with X-ray emission in a LHDAC.

A gradual spin transition of iron occurs over a P-T range extending from 1000 km and 1900 K to 2200 km and 2300 K in the lower mantle.

As low-spin ferropericlase exhibits higher density and faster sound velocities relative to the high-spin state ferropericlase, the increase in low-spin (Mg,Fe)O in the lower mantle would manifest seismically as a spin transition zone characterized by a steeper-than-normal density gradient.

Spin transition in lower mantle phases including perovskite and post-perovskite would have substantial effect on dynamics and chemistry in the lower mantle